RSC Advances

PAPER

View Article Online
View Journal | View Issue

Cite this: *RSC Adv.*, 2015, **5**, 12571

Tuned magnetism–luminescence bifunctionality simultaneously assembled into flexible Janus nanofiber

Fei Bi, Xiangting Dong,* Jinxian Wang and Guixia Liu

Received 8th September 2014
Accepted 22nd December 2014

DOI: 10.1039/c4ra10022k

www.rsc.org/advances

A new structure of [$CoFe_2O_4$/PVP]//[YAG:5%Eu^{3+}/PVP] magnetic–luminescent bifunctional Janus nanofibers has been successfully fabricated *via* electrospinning technology using a homemade parallel spinneret. Electrospinning-derived YAG:5%Eu^{3+} luminescent nanofibers and $CoFe_2O_4$ magnetic nanofibers are incorporated into polyvinyl pyrrolidone (PVP) matrix and electrospun into Janus nanofibers with $CoFe_2O_4$ magnetic nanofibers/PVP as one strand nanofiber and YAG:5%Eu^{3+} luminescent nanofibers/PVP as another strand nanofiber. [$CoFe_2O_4$/PVP]//[YAG:5%Eu^{3+}/PVP] magnetic–luminescent bifunctional Janus nanofibers possess superior magnetic and luminescent properties due to their special nanostructure, and the luminescent characteristics and saturation magnetizations of the Janus nanofibers can be tuned by adding various amounts of YAG:5%Eu^{3+} luminescent nanofibers and $CoFe_2O_4$ magnetic nanofibers. Compared with $CoFe_2O_4$/YAG:5%Eu^{3+}/PVP composite nanofibers, the magnetic–luminescent bifunctional Janus nanofibers provide higher performances due to the isolation of YAG:5%Eu^{3+} luminescent nanofibers from $CoFe_2O_4$ magnetic nanofibers. More importantly, the design conception and construction technology are of universal significance to fabricate other bifunctional Janus nanofibers.

1 Introduction

Nowadays, the development of the magnetic–luminescent bifunctional nanomaterials has attracted particular interest because of their wide applications in biological systems such as diagnostic analysis and controlled drug release.[1–5] Most of the magnetic–luminescent nanomaterials are core–shell structures. In general, organic dyes and quantum dots (QDs) have been used as the luminescence shell of the core–shell structured magnetic–luminescent nanomaterials.[6–9] However, the photobleaching and quenching properties of organic dyes and the toxicity of QDs have seriously limited their applications. Compared with organic dyes and QDs, lanthanide-doped nanomaterials have begun to attract attention due to their excellent luminescence properties. Among these luminescent materials, Eu^{3+}-activated $Y_3Al_5O_{12}$ (YAG) is an important phosphor with a variety of applications in many luminescent and optical devices due to its excellent performance.[10–13] As a type of magnetic material, cobalt ferrite ($CoFe_2O_4$) has received considerable attention because of its moderate saturation magnetization, high coercivity and excellent physical and chemical stability, as well as because of its potential applications in electronic devices, drug delivery technology, magnetic resonance imaging, and information storage.[14–16]

Presently, researchers are mainly focused on the preparation, properties and applications of magnetic–luminescent bifunctional nanoparticles. To obtain new morphologies of magnetic–luminescent nanomaterials, the fabrication of one-dimensional (1D) magnetic–luminescent nanomaterials is an urgent subject of study.

Electrospinning is a simple and versatile technique to process polymers and related materials into one-dimensional structural fibers with controllable compositions, diameters, and porosities for a variety of applications. This method not only has attracted extensive academic investigations, but it is also been applied in many areas.[17,18] To date, various magnetic–luminescent bifunctional 1D nanomaterials have been prepared *via* electrospinning.[19–21] From these studies, it has been proved that the existence of dark-colored magnetic nanomaterials greatly decreases the luminescence of rare earth compounds if magnetic nanomaterials are directly blended with the rare earth luminescent compounds.[22–26] Therefore, if the strong luminescence of the magnetic–luminescent bifunctional nanomaterials is to be achieved, rare earth compounds must be effectively isolated from magnetic nanomaterials to avoid their direct contact. In the procedure of seeking a way to ultimately reduce the impact of magnetic nanomaterials on the luminescent properties of the magnetic–luminescent bifunctional nanofibers, we were inspired by the reports about the Janus particles.[27–29] Janus particles have two distinguished

Key Laboratory of Applied Chemistry and Nanotechnology at Universities of Jilin Province, Changchun University of Science and Technology, Changchun 130022, China. E-mail: dongxiangting888@163.com; Fax: +86 0431 85383815; Tel: +86 0431 85582574

surfaces/chemistries on their two sides. Pierre-Gilles de Gennes, a winner of the Nobel Prize in Physics, introduced the Janus particles to the scientific community. These Janus-type morphologies allow the control of composition and surface anisotropy, providing additional degrees of freedom in the design of composite materials. Adopting the unique feature of the asymmetry dual-sided Janus structure, Janus nanofibers can successfully help to realize the effective separation of magnetic nanomaterials from rare earth luminescent compounds, and it is expected that the Janus nanofibers simultaneously exhibit both excellent magnetic and luminescent properties.

In this study, we designed and fabricated magnetic–luminescent bifunctional [$CoFe_2O_4$/PVP]//[YAG:5%Eu^{3+}/PVP] Janus nanofibers *via* electrospinning using a homemade spinneret. This Janus nanostructure can successfully realize the effective separation of $CoFe_2O_4$ nanofibers from YAG:5%Eu^{3+} nanofibers. The structure, morphology, luminescence characteristics and magnetic properties of the [$CoFe_2O_4$/PVP]//[YAG:5%Eu^{3+}/PVP] Janus nanofibers were investigated in detail, and some meaningful results were obtained.

2 Experimental section

2.1 Chemicals

Polyvinyl pyrrolidone (PVP, M_w = 1 300 000) and *N*,*N*-dimethylformamide (DMF) were purchased from Tianjin Tiantai Fine Chemical Reagents Co., Ltd. HNO_3 was bought from Beijing Chemical Company. Y_2O_3 (99.99%), Eu_2O_3 (99.99%), $Al(NO_3)_3\cdot 9H_2O$, $Fe(NO_3)_3\cdot 9H_2O$ and $Co(NO_3)_2\cdot 6H_2O$ were bought from Sinopharm Chemical Reagent Co., Ltd. All chemicals were of analytical grade and directly used as received without further purification. $Y(NO_3)_3\cdot 6H_2O$ and $Eu(NO_3)_3\cdot 6H_2O$ were prepared by dissolving Y_2O_3 and Eu_2O_3 in dilute nitric acid, followed by crystallizing from the solution through evaporating the excess water and HNO_3 by heating.

2.2 Preparation of $CoFe_2O_4$ nanofibers and YAG:5%Eu^{3+} nanofibers

A traditional single-spinneret electrospinning instrument was used to prepare $CoFe_2O_4$ nanofibers (named S_1) and YAG:5%Eu^{3+} nanofibers (named S_2). In a typical procedure of preparing spinning solution for fabricating $CoFe_2O_4$ nanofibers, 1 mmol of $Fe(NO_3)_3\cdot 9H_2O$, 0.5 mmol of $Co(NO_3)_2\cdot 6H_2O$ and 2.2 g of PVP were dissolved in 15.8 g of DMF with continuous stirring. The spinning solution for preparing YAG:5%Eu^{3+} nanofibers was prepared as follows: 0.95 mmol of $Y(NO_3)_3\cdot 6H_2O$, 0.05 mmol of $Eu(NO_3)_3\cdot 6H_2O$, 1.38 g of $Al(NO_3)_3\cdot 9H_2O$ and 2.4 g of PVP were added in 15.6 g of DMF to form a uniform solution with vigorous stirring. The spinning solutions were stirred for 4 h to form homogeneous mixture solutions for next-step electrospinning. Then, the spinning solutions were respectively injected into a traditional single-spinneret electrospinning setup, [$Fe(NO_3)_3$ + $Co(NO_3)_2$]/PVP composite nanofibers and [$Y(NO_3)_3$ + $Al(NO_3)_3$ + $Eu(NO_3)_3$]/PVP composite nanofibers were respectively prepared by electrospinning. The electrospinning parameters were as follows: the distance between the spinneret (a plastic needle) and collector was fixed at 18–20 cm and high voltage power supply was maintained at 12–15 kV. The room temperature was 20–24 °C and the relative humidity was 60%–70%. YAG:5%Eu^{3+} nanofibers and $CoFe_2O_4$ nanofibers could be obtained when the relevant composite nanofibers were annealed in air at 900 °C for 8 h and 700 °C for 4 h with a heating rate of 1 °C min^{-1}, respectively.

2.3 Fabrication of [$CoFe_2O_4$/PVP]//[YAG:5%Eu^{3+}/PVP] Janus nanofibers and $CoFe_2O_4$/YAG:5%Eu^{3+}/PVP composite nanofibers

Two different types of spinning solutions were prepared to fabricate Janus nanofibers. The spinning solution for preparing the strand $CoFe_2O_4$/PVP fiber of the Janus nanofibers was developed as follows: $CoFe_2O_4$ magnetic nanofibers (S_1) were ultrasonically dispersed in DMF for 20 min at room temperature, then a certain amount of PVP was added into the abovementioned mixture with stirring for 12 h, and the final mixture was denoted as spinning solution A. In the preparation of spinning solution for fabricating the strand YAG:5%Eu^{3+}/PVP fiber of the Janus nanofibers, YAG:5%Eu^{3+} luminescent nanofibers (S_2) were added into DMF, followed by ultrasonic dispersion for 20 min. Then, a certain amount of PVP was dissolved in the abovementioned solution with stirring for 12 h. A

Table 1 Compositions of the spinning solutions A and B

Samples	Spinning solutions	PVP/g	DMF/g	$CoFe_2O_4$ nanofibers (S_1)/g	YAG:5%Eu^{3+} nanofibers (S_2)/g
S_{a1}	A1 ($CoFe_2O_4$/PVP = 1 : 1)	0.300	2.007	0.300	
	B1 (YAG:5%Eu^{3+}/PVP = 1 : 1)	0.300	2.200		0.300
S_{a2}	A2 ($CoFe_2O_4$/PVP = 1 : 3)	0.900	6.023	0.300	
	B1 (YAG:5%Eu^{3+}/PVP = 1 : 1)	0.300	2.200		0.300
S_{a3}	A3 ($CoFe_2O_4$/PVP = 1 : 5)	1.500	10.035	0.300	
	B1 (YAG:5%Eu^{3+}/PVP = 1 : 1)	0.300	2.200		0.300
S_{a4}	A1 ($CoFe_2O_4$/PVP = 1 : 1)	0.300	2.007	0.300	
	B2 (YAG:5%Eu^{3+}/PVP = 1 : 2)	0.600	4.400		0.300
S_{a5}	A1 ($CoFe_2O_4$/PVP = 1 : 1)	0.300	2.007	0.300	
	B3 (YAG:5%Eu^{3+}/PVP = 1 : 3)	0.900	6.600		0.300
S_{a6}	A1 ($CoFe_2O_4$/PVP = 1 : 1)	0.300	2.007	0.300	
	B4 (YAG:5%Eu^{3+}/PVP = 1 : 5)	1.500	11.000		0.300
S_{b1}	Mixing A1 and B1	0.600	4.207	0.300	0.300

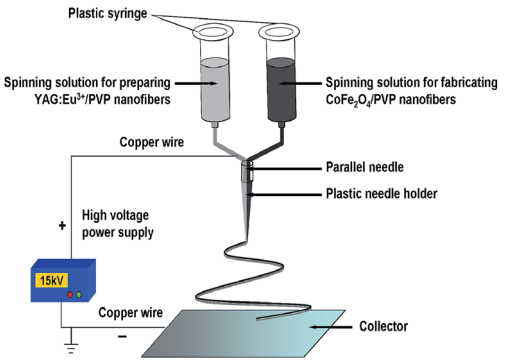

Fig. 1 Schematic diagram of the homemade parallel spinneret and the electrospinning setup.

mixed solution of YAG:5%Eu^{3+} nanofibers, PVP and DMF was prepared as the spinning solution B. The dosages of these materials are shown in Table 1.

[$CoFe_2O_4$/PVP]//[YAG:5%Eu^{3+}/PVP] Janus nanofibers were prepared using an electrospinning setup with a homemade parallel spinneret, as indicated in Fig. 1. The two types of spinning solutions were respectively loaded into each syringe, and the spinneret was vertically settled. A piece of flat iron net used as a collector was placed about 18 cm away from the tip of the plastic nozzle to collect the Janus nanofibers. A positive direct current (DC) voltage of 15 kV was applied between the spinneret and the collector. The electrospinning process was carried out at an ambient temperature of 22–24 °C and a relative air humidity of 60%–70%.

In addition, $CoFe_2O_4$/YAG:5%Eu^{3+}/PVP composite nanofibers (named S_{b1}, as shown in Table 1), as a contrast sample, were also prepared to study the superiority of the structure of Janus nanofibers. $CoFe_2O_4$/YAG:5%Eu^{3+}/PVP composite nanofibers were fabricated by mixing the spinning solution A1 ($CoFe_2O_4$/PVP = 1 : 1) and the spinning solution B1 (YAG:5%Eu^{3+}/PVP = 1 : 1) together using a traditional single-spinneret electrospinning setup, and the spinning parameters were the same as those in the fabrication of the Janus nanofibers.

3 Characterization

The samples were identified by an X-ray powder diffractometer (XRD, Bruker D8 FOCUS) with Cu Kα radiation, and the operation voltage and current were kept at 40 kV and 20 mA, respectively. The morphology and internal structure of samples were observed by a field emission scanning electron microscope (SEM, XL-30) and a transmission electron microscope (TEM, JEM-2010), respectively. The luminescent properties of the samples were investigated by a Hitachi fluorescence spectrophotometer F-7000. The magnetic performance of the samples was measured by a vibrating sample magnetometer (VSM, MPMS SQUID XL). The ultraviolet-visible diffuse reflectance spectrum of the samples was determined by a UV-1240 ultraviolet-visible spectrophotometer. All the measurements were performed at room temperature.

4 Results and discussion

4.1 Crystal structure

The phase compositions of [$CoFe_2O_4$/PVP]//[YAG:5%Eu^{3+}/PVP] Janus nanofibers (S_{a1}) and $CoFe_2O_4$/YAG:5%Eu^{3+}/PVP composite nanofibers (S_{b1}) were characterized using XRD analysis, as shown in Fig. 2. It can be seen that XRD patterns of [$CoFe_2O_4$/PVP]//[YAG:5%Eu^{3+}/PVP] Janus nanofibers and $CoFe_2O_4$/YAG:5%Eu^{3+}/PVP composite nanofibers are conformed to the cubic phase with a primitive structure of YAG (PDF#33-0040) and the cubic spinel structure of $CoFe_2O_4$ (PDF#22-1086), and the diffraction peak of the amorphous PVP (2θ = 22.2°) also can be observed, indicating that [$CoFe_2O_4$/PVP]//[YAG:5%Eu^{3+}/PVP] Janus nanofibers and $CoFe_2O_4$/YAG:5%Eu^{3+}/PVP composite nanofibers contain crystalline YAG:7%Tb^{3+}, $CoFe_2O_4$ and amorphous PVP.

4.2 Morphology

The morphologies of the as-prepared $CoFe_2O_4$ nanofibers (S_1) and YAG:5%Eu^{3+} nanofibers (S_2) were observed by means of SEM, as presented in Fig. 3a and b. $CoFe_2O_4$ nanofibers and YAG:5%Eu^{3+} nanofibers have coarse surfaces, the size distribution of the as-prepared nanofibers are almost uniform, and the diameters of the $CoFe_2O_4$ nanofibers and YAG:5%Eu^{3+} nanofibers are 81.43 ± 9.2 nm and 126.84 ± 16.9 nm at the confidence level of 95%, respectively, as demonstrated in Fig. 4a and b. The morphologies and structures of [$CoFe_2O_4$/PVP]//[YAG:5%Eu^{3+}/PVP] Janus nanofibers (S_{a1}) and $CoFe_2O_4$/YAG:5%Eu^{3+}/PVP composite nanofibers (S_{b1}) were characterized by the combination of SEM and TEM analyses. As seen from Fig. 3c–e, the surface of the Janus nanofibers and composite nanofibers is smooth, and each [$CoFe_2O_4$/PVP]//[YAG:5%Eu^{3+}/PVP] Janus nanofiber consists of two nanofibers assembled side-by-side. A TEM image of [$CoFe_2O_4$/PVP]//[YAG:5%Eu^{3+}/PVP] Janus nanofibers is presented in Fig. 3f. One strand nanofiber of the Janus nanofiber is composed of $CoFe_2O_4$ magnetic nanofibers and PVP, and the other one consists of YAG:5%Eu^{3+} luminescent nanofibers and PVP. The mean diameter of an individual nanofiber of the Janus nanofibers (S_{a1}) is *ca.* 283.06 ± 36.7 nm at the confidence level of 95%, as revealed in Fig. 4c. It can be observed from Fig. 3g

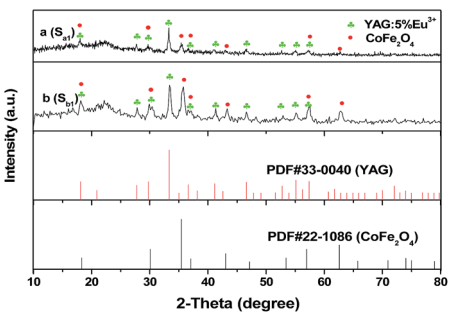

Fig. 2 XRD patterns of [$CoFe_2O_4$/PVP]//[YAG:5%Eu^{3+}/PVP] Janus nanofibers (S_{a1}) (a) and $CoFe_2O_4$/YAG:5%Eu^{3+}/PVP composite nanofibers (S_{b1}) (b) with PDF standard cards of YAG and $CoFe_2O_4$.

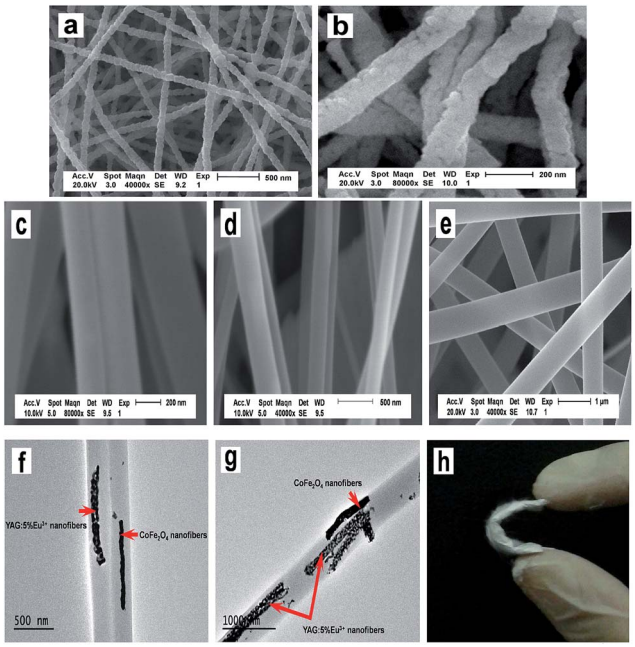

Fig. 3 SEM images of $CoFe_2O_4$ nanofibers (S_1) (a), YAG:5%Eu^{3+} nanofibers (S_2) (b), and SEM and TEM images of [$CoFe_2O_4$/PVP]//[YAG:5%Eu^{3+}/PVP] Janus nanofibers (S_{a1}) (c–e), $CoFe_2O_4$/YAG:5%Eu^{3+}/PVP composite nanofibers (S_{b1}) (f and g) and a digital image of [$CoFe_2O_4$/PVP]//[YAG:5%Eu^{3+}/PVP] flexible Janus nanofibers (h).

that $CoFe_2O_4$ magnetic nanofibers and YAG:5%Eu^{3+} luminescent nanofibers are dispersed in the $CoFe_2O_4$/YAG:5%Eu^{3+}/PVP composite nanofibers. The diameter of the $CoFe_2O_4$/YAG:5%Eu^{3+}/PVP composite nanofibers (S_{b1}) is 632.98 ± 33.6 nm at the confidence level of 95%, as revealed in Fig. 4d. From the abovementioned SEM and TEM analyses, we can confirm that the [$CoFe_2O_4$/PVP]//[YAG:5%Eu^{3+}/PVP] Janus nanofibers have been successfully fabricated. As seen in Fig. 3h, the Janus nanofibers are flexible nanofibers.

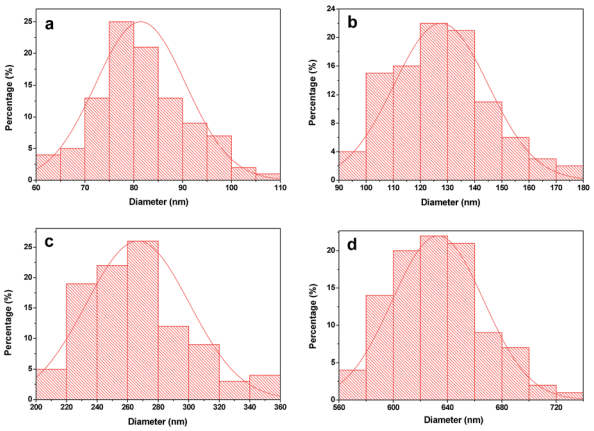

Fig. 4 Histograms of diameter distribution of $CoFe_2O_4$ nanofibers (S_1) (a), YAG:5%Eu^{3+} nanofibers (S_2) (b), [$CoFe_2O_4$/PVP]//[YAG:5%Eu^{3+}/PVP] Janus nanofibers (S_{a1}) (c) and $CoFe_2O_4$/YAG:5%Eu^{3+}/PVP composite nanofibers (S_{b1}) (d).

4.3 Luminescent properties of [$CoFe_2O_4$/PVP]//[YAG:5%Eu^{3+}/PVP] Janus nanofibers

To investigate the impact of the mass ratio of YAG:5%Eu^{3+} luminescent nanofibers to PVP on the luminescent performance, a series of [$CoFe_2O_4$/PVP]//[YAG:5%Eu^{3+}/PVP] Janus nanofibers (S_{a1}, S_{a4}, S_{a5} and S_{a6}) were fabricated. To perform this study, the mass ratio of $CoFe_2O_4$ nanofibers to PVP was fixed at 1 : 1 and the mass ratio of YAG:5%Eu^{3+} nanofibers to PVP was varied from 1 : 1 to 1 : 5. It can be observed from Fig. 5a that the excitation spectra (monitored by 591 nm) of the samples show a predominant excitation band (200–300 nm) centered at 235 nm, which is assigned to the charge transfer from the 2p orbital of O^{2-} ions to the 4f orbital of Eu^{3+} ions, while the sharp excitation peak at 391 nm is due to the $^7F_0 \rightarrow {}^5L_6$ transition of Eu^{3+} ions. As shown in Fig. 5b, characteristic emission peaks of Eu^{3+} are observed under the excitation of 235 nm ultraviolet light and ascribed to the energy levels transitions of $^5D_0 \rightarrow {}^7F_1$ (591 nm), $^5D_0 \rightarrow {}^7F_1$ (597 nm), $^5D_0 \rightarrow {}^7F_2$ (611 nm) and $^5D_0 \rightarrow {}^7F_2$ (631 nm) of Eu^{3+} ions. The $^5D_0 \rightarrow {}^7F_1$ energy level transition at 591 nm is the predominant emission peak. It is found from Fig. 5 that the peaks have the same spectral shape when the amount of luminescent substance increases, whereas the intensities of the excitation and emission peaks are strengthened, indicating that the luminescent intensity of the Janus nanofibers can be tuned by adjusting the amount of luminescent material.

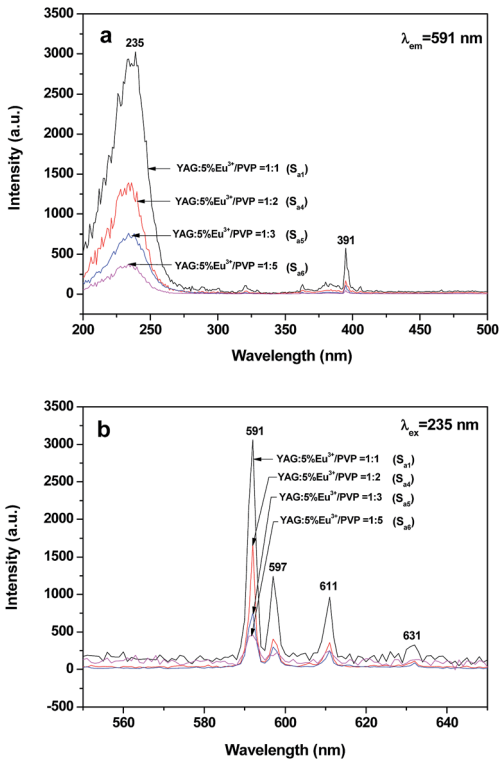

Fig. 5 Excitation spectra (a) and emission spectra (b) of [$CoFe_2O_4$/PVP]//[YAG:5%Eu^{3+}/PVP] Janus nanofibers (S_{a1}, S_{a4}, S_{a5} and S_{a6}) containing different mass ratios of YAG:5%Eu^{3+} nanofibers to PVP when the mass ratio of $CoFe_2O_4$ nanofibers to PVP is fixed at 1 : 1.

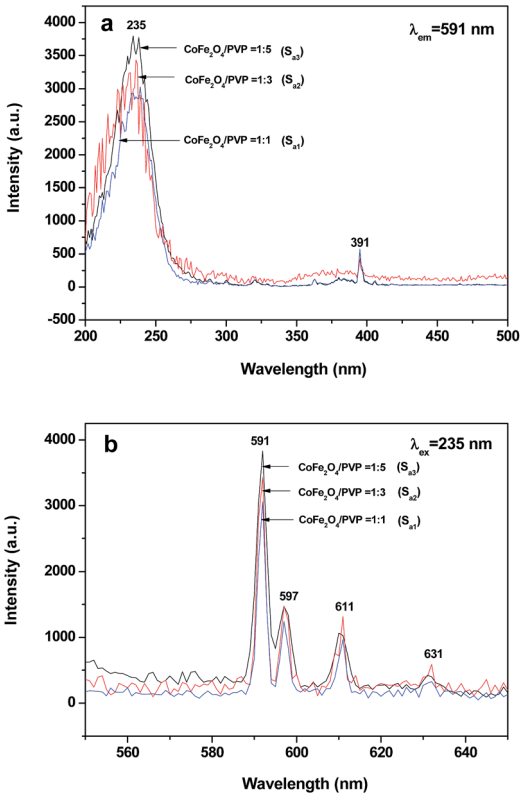

Fig. 6 Excitation spectra (a) and emission spectra (b) of [$CoFe_2O_4$/PVP]//[YAG:5%Eu^{3+}/PVP] Janus nanofibers (S_{a1}, S_{a2} and S_{a3}) containing different mass ratios of $CoFe_2O_4$ nanofibers to PVP when the mass ratio of YAG:5%Eu^{3+} to PVP is fixed at 1 : 1.

The excitation spectra (monitored at 591 nm) and emission spectra (excited by 235 nm) of [$CoFe_2O_4$/PVP]//[YAG:5%Eu^{3+}/PVP] Janus nanofibers (S_{a1}, S_{a2} and S_{a3}) containing different amounts of $CoFe_2O_4$ magnetic nanofibers are indicated in Fig. 6. To perform this investigation, the mass ratio of YAG:5% Eu^{3+} nanofibers to PVP was fixed at 1 : 1 and the mass ratio of $CoFe_2O_4$ nanofibers to PVP was varied from 1 : 1 to 1 : 5. As seen from Fig. 6, the excitation and emission intensity of [$CoFe_2O_4$/PVP]//[YAG:5%Eu^{3+}/PVP] Janus nanofibers decreased with the increasing amount of $CoFe_2O_4$ nanofibers introduced into the Janus nanofibers. This phenomenon may result from the light absorbance of the dark-colored $CoFe_2O_4$ nanofibers. From the ultraviolet-visible diffuse reflectance spectrum of $CoFe_2O_4$ nanofibers (S_1) illustrated in Fig. 7, it is observed that $CoFe_2O_4$ nanofibers can absorb light at ultraviolet wavelengths (<400 nm) much more strongly than in the visible range (400–700 nm). Both the exciting light (235 nm) and emitting light (591–631 nm) can be absorbed by dark-colored $CoFe_2O_4$. Thus, the exciting light and emitting light are absorbed by the $CoFe_2O_4$ nanofibers, resulting in the decrease in the intensity of excitation and emission peaks. Furthermore, more the $CoFe_2O_4$ nanofibers are introduced into the Janus nanofibers, more the decrease in the intensity of excitation and emission peaks occurs.

To illustrate the advantages of the nanostructure of the magnetic–luminescent bifunctional Janus nanofibers, $CoFe_2O_4$/YAG:5%Eu^{3+}/PVP composite nanofibers (S_{b1}), as a contrast sample, were also fabricated by mixing the spinning solution A1 ($CoFe_2O_4$/PVP = 1 : 1) and the spinning solution B1 (YAG:5% Eu^{3+}/PVP = 1 : 1) together, followed by electrospinning *via* the traditional single-spinneret electrospinning setup. From the contrast between the Janus nanofibers (S_{a1}) ($CoFe_2O_4$/PVP = 1 : 1, YAG:5%Eu^{3+}/PVP = 1 : 1) and $CoFe_2O_4$/YAG:5%Eu^{3+}/PVP composite nanofibers (S_{b1}), which have the same components, as shown in Fig. 8, one can see that the emission intensity of the Janus nanofibers is considerably stronger than that of $CoFe_2O_4$/YAG:5%Eu^{3+}/PVP composite nanofibers. This result can be attributed to the isolation of YAG:5%Eu^{3+} from $CoFe_2O_4$. As illustrated in Fig. 9, YAG:5%Eu^{3+} nanofibers and $CoFe_2O_4$ nanofibers are promiscuously dispersed in the $CoFe_2O_4$/YAG:5%Eu^{3+}/PVP composite nanofiber. The exciting light in the composite nanofiber has to pass through $CoFe_2O_4$ nanofibers to reach and excite YAG:5%Eu^{3+} nanofibers. In this process, a large part of the exciting light is absorbed by $CoFe_2O_4$ nanofibers, and thus the exciting light is considerably weakened before it reaches the YAG:5%Eu^{3+} nanofibers. Similarly, the emitting light emitted by YAG:5%Eu^{3+} nanofibers also has to pass through $CoFe_2O_4$ nanofibers and is absorbed by them.

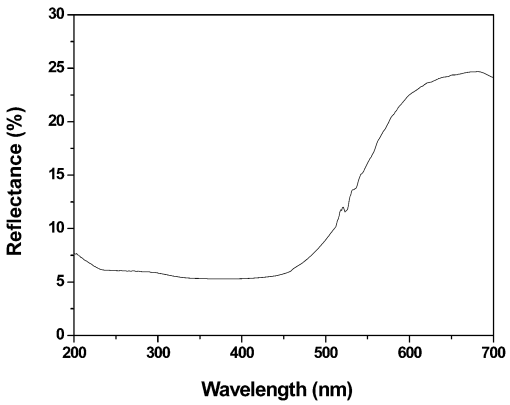

Fig. 7 UV-vis diffuse reflectance spectrum of $CoFe_2O_4$ nanofibers (S_1).

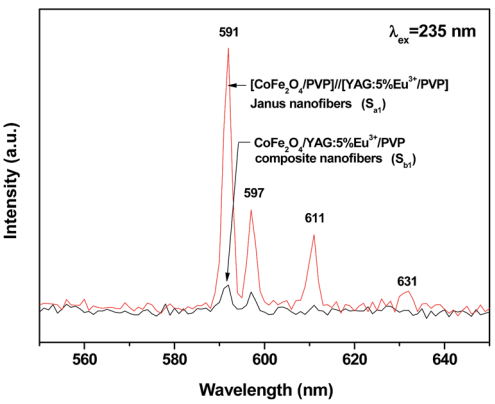

Fig. 8 Emission spectra of [$CoFe_2O_4$/PVP]//[YAG:5%Eu^{3+}/PVP] Janus nanofibers (S_{a1}) and $CoFe_2O_4$/YAG:5%Eu^{3+}/PVP composite nanofibers (S_{b1}).

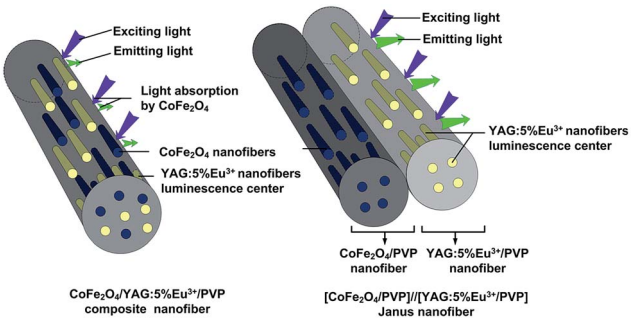

Fig. 9 Schematic diagram of the situation of the exciting light and emitting light in $CoFe_2O_4$/YAG:5%Eu^{3+}/PVP composite nanofibers and [$CoFe_2O_4$/PVP]//[YAG:5%Eu^{3+}/PVP] Janus nanofibers.

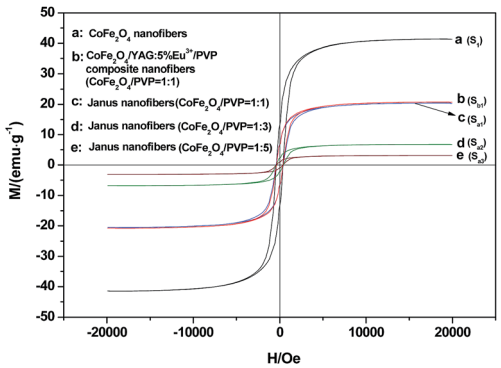

Fig. 10 Hysteresis loops of $CoFe_2O_4$ nanofibers (S_1) (a), $CoFe_2O_4$/YAG:5%Eu^{3+}/PVP composite nanofibers (S_{b1}) (b) and [$CoFe_2O_4$/PVP]//[YAG:5%Eu^{3+}/PVP] Janus nanofibers (S_{a1}, S_{a2} and S_{a3}) containing different mass ratios of $CoFe_2O_4$ nanofibers to PVP (c–e).

Consequently, both the exciting and emitting light are severely weakened. For [$CoFe_2O_4$/PVP]//[YAG:5%Eu^{3+}/PVP] Janus nanofibers, YAG:5%Eu^{3+} nanofibers and $CoFe_2O_4$ nanofibers are separated in their own strand, so that the exciting light and emitting light in the YAG:5%Eu^{3+} nanofibers strand will be little affected by $CoFe_2O_4$ nanofibers. The overall effect is that the [$CoFe_2O_4$/PVP]//[YAG:5%Eu^{3+}/PVP] Janus nanofibers possess much higher luminescent performance than the $CoFe_2O_4$/YAG:5%Eu^{3+}/PVP composite nanofibers.

4.4 Magnetic properties of [$CoFe_2O_4$/PVP]//[YAG:5%Eu^{3+}/PVP] Janus nanofibers

The typical hysteresis loops for $CoFe_2O_4$ nanofibers (S_1), [$CoFe_2O_4$/PVP]//[YAG:5%Eu^{3+}/PVP] Janus nanofibers (S_{a1}, S_{a2} and S_{a3}) containing different mass ratios of $CoFe_2O_4$ nanofibers to PVP and $CoFe_2O_4$/YAG:5%Eu^{3+}/PVP composite nanofibers (S_{b1}) are shown in Fig. 10, and the saturation magnetizations of the samples are summarized in Table 2. As seen from Fig. 10, the saturation magnetization of the $CoFe_2O_4$ nanofibers is 41.34 emu g^{-1}, which is similar to the data reported by previous studies[14–16]. The saturation magnetization of [$CoFe_2O_4$/PVP]//[YAG:5%Eu^{3+}/PVP] Janus nanofibers containing different mass ratios of $CoFe_2O_4$ nanofibers to PVP are 20.32 emu g^{-1}, 6.73 emu g^{-1} and 3.12 emu g^{-1}, as revealed in Fig. 10 and Table 2. It is known that the saturation magnetization of a magnetic composite material depends on the mass percentage of the magnetic substance in the magnetic composite material.[21–23] It is found that the saturation magnetization of the [$CoFe_2O_4$/PVP]//[YAG:5%Eu^{3+}/PVP] Janus nanofibers is increased with the amount of $CoFe_2O_4$ magnetic nanofibers introduced into the $CoFe_2O_4$/PVP strand, implying that the magnetism of the Janus nanofibers can be tunable by adjusting the amount of $CoFe_2O_4$ magnetic nanofibers. The saturation magnetization of the $CoFe_2O_4$/YAG:5%Eu^{3+}/PVP composite nanofibers is 20.53 emu g^{-1}, which is close to that of the Janus nanofibers marked c (20.32 emu g^{-1}) in Fig. 10. Combining luminescence with magnetism analysis, it is found that when the Janus nanofibers have a close magnetic property to the $CoFe_2O_4$/YAG:5%Eu^{3+}/PVP composite nanofibers, the luminescent intensity of the Janus nanofibers is considerably higher than that of the composite nanofibers, demonstrating that the novel Janus nanofibers have better magnetic–luminescent performance than the composite nanofibers.

5 Conclusions

In summary, magnetic–luminescent bifunctional [$CoFe_2O_4$/PVP]//[YAG:5%Eu^{3+}/PVP] Janus nanofibers have been successfully synthesized by electrospinning technology using a home-made parallel spinneret. One strand nanofiber of the Janus nanofiber is composed of $CoFe_2O_4$ magnetic nanofibers and PVP, and the other one consists of YAG:5%Eu^{3+} luminescent nanofibers and PVP. The average diameter of each strand of the Janus nanofiber is *ca.* 283.06 ± 36.7 nm. It is very gratifying to see that the magnetic–luminescent bifunctional Janus nanofibers simultaneously possess both excellent luminescent performance and magnetic properties. Furthermore, the luminescent intensity and magnetism of the Janus nanofibers can be tuned *via* adjusting the content of luminescent and magnetic compounds. In addition, the design conception and

Table 2 Saturation magnetization of samples

Samples	Saturation magnetization (M_s)/(emu g^{-1})
$CoFe_2O_4$ nanofibers (S_1)	41.34
$CoFe_2O_4$/YAG:5%Eu^{3+}/PVP composite nanofibers (S_{b1}) ($CoFe_2O_4$/PVP = 1 : 1)	20.53
[$CoFe_2O_4$/PVP]//[YAG:5%Eu^{3+}/PVP] Janus nanofibers (S_{a1}) ($CoFe_2O_4$/PVP = 1 : 1)	20.32
[$CoFe_2O_4$/PVP]//[YAG:5%Eu^{3+}/PVP] Janus nanofibers (S_{a2}) ($CoFe_2O_4$/PVP = 1 : 3)	6.73
[$CoFe_2O_4$/PVP]//[YAG:5%Eu^{3+}/PVP] Janus nanofibers (S_{a3}) ($CoFe_2O_4$/PVP = 1 : 5)	3.12

preparation method of the Janus nanofibers are of universal significance to fabricate other one-dimensional multifunctional nanostructures. The new high-performance [$CoFe_2O_4$/PVP]// [YAG:5%Eu^{3+}/PVP] magnetic–luminescent bifunctional Janus nanofibers have potential applications in the fields of medical diagnostics, drug target delivery, optical imaging, anti-counterfeiting technology and future nanomechanics.

Acknowledgements

This work was financially supported by the National Natural Science Foundation of China (NSFC 50972020, 51072026), Specialized Research Fund for the Doctoral Program of Higher Education (20102216110002, 20112216120003), the Science and Technology Development Planning Project of Jilin Province (Grant nos 20130101001JC, 20070402), the Science and Technology Research Project of the Education Department of Jilin Province during the eleventh five-year plan period (Under grant no 2010JYT01), Key Research Project of Science and Technology of Ministry of Education of China (Grant no 207026).

Notes and references

1 W. Wang, Z. Y. Li, X. R. Xu, B. Dong, H. N. Zhang, Z. J. Wang, C. Wang, R. H. Baughman and S. L. Fang, *Small*, 2011, **7**, 597.
2 W. Wang, M. Zou and K. Z. Chen, *Chem. Commun.*, 2010, **46**, 5100.
3 J. Feng, S. Y. Song, R. P. Deng, W. Q. Fan and H. J. Zhang, *Langmuir*, 2010, **26**, 3596.
4 H. Y. Chen, D. C. Colvin, B. Qi, T. Moore, J. He, O. T. Mefford, F. Alexis, J. C. Gore and J. N. Anker, *J. Mater. Chem.*, 2012, **22**, 12802.
5 P. Lu, J. L. Zhang, Y. L. Liu, D. H. Sun, G. X. Liu, G. Y. Hong and J. Z. Ni, *Talanta*, 2010, **83**, 450.
6 H. G. Wang, L. Sun, Y. P. Li, X. L. Fei, M. D. Sun, C. Q. Zhang, Y. X. Li and Q. B. Yang, *Langmuir*, 2011, **27**, 11609.
7 P. Sun, H. Y. Zhang, C. Liu, J. Fang, M. Wang, J. Chen, J. P. Zhang, C. B. Mao and S. K. Xu, *Langmuir*, 2010, **26**, 1278.
8 F. Grasset, F. Dorson, Y. Molard, S. Cordier, V. Demange, C. Perrin, V. Marchi-Artzner and H. Haneda, *Chem. Commun.*, 2008, **39**, 4729.
9 L. N. Chen, J. Wang, W. T. Li and H. Y. Han, *Chem. Commun.*, 2012, **48**, 4971.
10 X. M. Li, X. Xing, W. J. Yang, W. L. Li and L. F. Kong, *Semiconductor Optoelectronics*, 2010, **31**, 71.
11 R. Lopez, E. A. Aguilar and J. Zarate-Medina, *J. Eur. Ceram. Soc.*, 2010, **30**, 73.
12 P. F. S. Pereira, M. G. Matos, L. R. Ávila, E. C. O. Nassor, A. Cestari, K. J. Ciuffi, P. S. Calefi and E. J. Nassar, *J. Lumin.*, 2010, **130**, 488.
13 H. K. Yang and J. H. Jeong, *J. Phys. Chem. C*, 2010, **114**, 226.
14 J. C. Fu, J. L. Zhang, Y. Peng, J. G. Zhao, G. G. Tan, N. J. Mellors, E. Q. Xie and W. H. Han, *Nanoscale*, 2012, **4**, 3932.
15 C. Fernandes, C. Pereira, M. P. F. García, A. M. Pereira, A. Guedes, R. F. Pacheco, A. Ibarra, M. R. Ibarra, J. P. Araújo and C. Freire, *J. Mater. Chem. C*, 2014, **2**, 5818.
16 Q. Cao, Z. W. Liu and R. C. Che, *New J. Chem.*, 2014, **38**, 3193.
17 H. Wang, Y. Li, L. Sun, Y. Li, W. Wang, S. Wang, S. Xu and Q. Yang, *J. Colloid Interface Sci.*, 2010, **350**, 396.
18 Z. Y. Hou, C. X. Li, P. G. Ma, G. G. Li, Z. Y. Cheng, C. Peng, D. M. Yang, P. P. Yang and J. Lin, *Adv. Funct. Mater.*, 2011, **21**, 2356.
19 J. B. Mu, C. L. Shao, Z. C. Guo, Z. Y. Zhang, M. Y. Zhang, P. Zhang, B. Chen and Y. C. Liu, *ACS Appl. Mater. Interfaces*, 2011, **3**, 590.
20 J. Song, M. L. Chen, M. B. Olesen, C. X. Wang, R. Havelund, Q. Li, E. Q. Xie, R. Yang, P. Bøggild, C. Wang, F. Besenbacher and M. D. Dong, *Nanoscale*, 2011, **3**, 4966.
21 N. Lv, Q. L. Ma, X. T. Dong, J. X. Wang, W. S. Yu and G. X. Liu, *Chem. Eng. J.*, 2014, **243**, 500.
22 S. L. Chen, H. Q. Hou, F. Harnisch, S. A. Patil and A. A. Carmona-Martinez, *Energy Environ. Sci.*, 2011, **4**, 1417.
23 N. Lv, Q. L. Ma, X. T. Dong, J. X. Wang, W. S. Yu and G. X. Liu, *ChemPlusChem*, 2014, **79**, 690.
24 Q. L. Ma, W. S. Yu, X. T. Dong, J. X. Wang and G. X. Liu, *Nanoscale*, 2014, **6**, 2945.
25 Q. L. Ma, J. X. Wang, X. T. Dong, W. S. Yu and G. X. Liu, *ChemPlusChem*, 2014, **79**, 290.
26 X. Xi, J. X. Wang, X. T. Dong, Q. L. Ma, W. S. Yu and G. X. Liu, *Chem. Eng. J.*, 2014, **254**, 259.
27 T. Nisisako, T. Torii, T. Takahashi and Y. Takizawa, *Adv. Mater.*, 2006, **18**, 1152.
28 H. R. Kyung, C. M. David and L. Joerg, *Nat. Mater.*, 2005, **4**, 759.
29 S. Isaac, Y. Xin, J. C. Emily, M. M. Nicholas, T. M. Gerald, K. Olga and C. B. Anna, *ACS Nano*, 2013, **7**, 1224.